

A Novel Electrochemical Sensor for Paracetamol Based on β -Cyclodextrin/Nafion[®]/Polymer Nanocomposite

Nada F. Atta^{1,*}, Ahmed Galal¹ and Dalia M. El-Said²

¹Department of Chemistry, Faculty of Science, Cairo University, 12613 Giza, Egypt.

²Forensic Chemistry Laboratories, Medico Legal Department, Ministry of Justice, Cairo, Egypt.

*E-mail: nada_fahl@yahoo.com

Received: 25 October 2014 / Accepted: 30 November 2014 / Published: 16 December 2014

A sensitive electrochemical sensor based on β -cyclodextrin/Nafion[®]/poly(3,4-ethylenedioxythiophene) nanocomposite modified gold electrode Au/PEDOT/NF/CD was fabricated for the determination of paracetamol ACOP in presence of interference compounds. Au/PEDOT/NF/CD showed an excellent electrocatalytic synergism between its components for the electrooxidation of ACOP. Conductive PEDOT polymer film acts as an electron mediator with a rich electron cloud. Furthermore nafion improves the electrical conductivity of the composite as well it works as suitable layer for the formation of the CD film over it due to its good adhesion at the polymer surface and good film forming ability. By the modification of Au/PEDOT/NF with CD film, enhanced charge transfer kinetics and improved oxidation current for ACOP were obtained. A supramolecular host-guest inclusion complex is formed between β -CD and ACOP via electrostatic, inclusion interactions and hydrogen bonds formation. The formation of such complex resulted in selective advantage and enhancement of the charge transfer properties of ACOP. ACOP molecules penetrate into the less polar cavity of β -CD and ACOP:CD inclusion complex was formed which further resulted in significant increase in oxidation signal of ACOP. Under optimized conditions a linear calibration curve was obtained for the determination of ACOP in urine within the range 3–300 $\mu\text{mol L}^{-1}$ with a correlation coefficient of 0.9958 and detection limit of 36.1 nmol L^{-1} . Simultaneous determinations of ACOP and epinephrine (EP), ACOP and norepinephrine (NE), ACOP, DA and AA and ACOP, EP and AA were achieved at the modified sensor with high resolution and good potential peak separation.

Keywords: Paracetamol; Nafion; Host-guest complex; Cyclodextrin; Electrochemical sensor; Synergism.

1. INTRODUCTION

Acetaminophen or paracetamol (ACOP), analgesic and anti-pyretic drug, is an effective, safe and suitable alternative when the patients are sensitive to aspirin [1, 2]. Acetaminophen is widely used in the case of fever cough, cold and mild to moderate pain including tension headache, migraine headache, muscular aches, chronic pain, neuralgia, backache, joint pain, general pain and toothache. It is also useful in osteoarthritis therapy and it is sometimes used for management of cancer pain [1-6]. Therefore, it is very important to construct a simple, fast, sensitive and accurate method for the determination of ACOP. Several approaches have been developed for the sensitive determination of ACOP such as gold nanoparticles and nafion modified carbon paste electrode [1, 2], Pd nanoclusters-coated polyfuran [3], Pd [4], zirconium nanoparticles [7] or multi-walled carbon nanotubes [8] modified graphene oxide, Nafion[®]/TiO₂ [5] or carbon nanotube modified graphene [9, 10], molecularly imprinted polymeric films [6, 11], nanostructured mesoporous materials [12] and multi-wall carbon nanotubes [13].

Conducting polymers exhibited fascinating properties for various applications especially as coating in fabrication of electro-sensors. Poly (3,4-ethylenedioxythiophene) (PEDOT) is the most studied one among the family of the polythiophenes [14, 15]. PEDOT presented optimistic advantages that make it very promising in the design of an electrochemical sensor. It has the ability to adhere well on most electrode materials, show high conductivity in its oxidized state, resists fouling by the oxidation products and present good stability in aqueous electrolytes and biocompatibility with biological media [16-21].

Nafion[®] (NF) is a per-fluorinated sulfonated cation exchanger which is highly permeable to cations but almost impermeable to anions. It consists of a linear backbone of fluorocarbon chains and ethyl ether pendant groups with sulfonic cation exchange sites. NF presented many advantages like high chemical and thermal stability, chemical inertness and mechanical strength. In addition, easy fabrication, good adhesion on the electrode surface, improvement of the anti-interferential ability of the sensor, high partition coefficients of many redox compounds in NF and good electrical conductivity make NF a fascinating material for the modification of electrodes in electrochemistry especially in biosensors [22-31]. The accumulation mechanism of NF can be achieved via an electrostatic interaction through the hydrophilic negatively charged sulfonate groups in the polymer structure. On the other hand, the ionic selectivity of NF toward hydrophobic organic cations is achieved via hydrophobic interactions with the hydrophobic fluorocarbons of the film [32, 33]. NF films allow the electrolytes to proceed while preventing adsorption-desorption processes of organic species. Also, NF preconcentrates positively charged molecules resulting in enhanced sensitivity of the measurements [32-37].

On the other hand, attractive structural characteristics and special functions were achieved with another electrode modifier belongs to the cyclodextrin family [38-42]. α -, β - and γ -cyclodextrins are cyclic oligosaccharides consisting of six, seven or eight glucose units [43-45]. CDs contained a hydrophobic inner cavity and a hydrophilic outer tail. CDs occupied large era in the design of selective electrodes as they had the ability to form stable and selective host-guest inclusion complexes with suitable organic, inorganic, neutral and ionic substances [46-52]. Especial attention was given to β -

cyclodextrin (CD) which is composed of α -1,4 linked glucopyranose subunit [46, 53-59]. It presented many advantages like good biocompatibility and adsorption capabilities directly on solid surfaces. Therefore, it was applied in different fields such as electrochemical sensor, catalysis, enzyme mimics, biological systems, molecular recognition and increasing solubility and dispersibility [53, 56-58].

The aim of this work is to investigate the electrochemical oxidation behavior of ACOP for the first time at Au/PEDOT/NF/CD composite electrode. Based on the effective synergism between PEDOT, CD and NF, the proposed sensor presented a good candidate for enhancing the oxidation current response of ACOP and facilitating its electron transfer rate. The performance of the fabricated electrode in terms of sensitivity, linear range and selectivity is evaluated and discussed. In addition, the simultaneous determinations of ACOP and epinephrine (EP), ACOP and norepinephrine (NE), ACOP, DA and AA and ACOP, EP and AA were investigated at the proposed sensor. Also, as real sample analysis, the applicability of this sensor for determination of ACOP in urine was achieved with excellent recovery results.

2. EXPERIMENTAL

2.1. Materials and reagents

All chemicals were used as received without further purification. 3,4-ethylene dioxy-thiophene (EDOT), tetrabutylammonium hexafluorophosphate (Bu_4NPF_6), acetonitrile ([HPLC] grade), lithium perchlorate (LiClO_4), paracetamol (ACOP), dopamine (DA), ascorbic acid (AA), epinephrine (EP), norepinephrine (NE), Nafion[®](NF) and β -cyclodextrin (CD) were supplied by Aldrich Chem. Co. (Milwaukee, WI, USA). Phosphate buffer solution 0.1 mol L⁻¹ PBS (1 mol L⁻¹ K_2HPO_4 and 1 mol L⁻¹ KH_2PO_4) was used as the supporting electrolyte. pH was adjusted using 0.1 mol L⁻¹ H_3PO_4 and 0.1 mol L⁻¹ KOH. All solutions were prepared using double distilled water.

2.2. Electrochemical cells and equipments

Electrochemical polymerization and characterization were carried out with a three electrode/one-compartment glass cell. It was connected to the electrochemical workstation from BAS-100B electrochemical analyzer (Bioanalytical Systems, BAS, West Lafayette, USA). The working electrode was gold disc (diameter: 1.5 mm). A 6.0 cm platinum wire from BAS was employed as auxiliary electrode. All the cell potentials were measured with respect to Ag/AgCl (4 mol L⁻¹ KCl saturated with AgCl) reference electrode from BAS. Working electrode was polished using alumina (2 μM)/water slurry until no visible scratches were observed. Prior to immersion in the cell, the electrode surface was thoroughly rinsed with distilled water and dried. All experiments were performed at 25 ± 0.2 °C. The electrochemical impedance spectroscopy was performed using a Gamry-750 system and a lock-in-amplifier that are connected to personal computer. The data analysis software was provided with the instrument and applied non linear least square fitting with Levenberg-Marquardt algorithm. All impedance experiments were recorded between 0.1 Hz and 100 kHz. Quanta FEG 250 instrument was used to obtain the scanning electron micrographs.

2.3. Construction of the proposed sensor

Bulk Electrolysis (BE) was employed for deposition of the polymer film from a solution of 0.001 M EDOT and 0.05 M Bu_4NPF_6 in acetonitrile. The potential applied between gold disc working electrode and the reference (Ag/AgCl) was held constant at +1.4 V for 10 s (the optimized time). The electrode was represented as Au/PEDOT. Then 10 μL (the optimized volume) of 2% nafion (NF) (the optimized concentration) was added on Au/PEDOT electrode. The electrode was left for 20 min in open air to allow the NF film to dry. The utilized electrode is represented as Au/PEDOT/NF. Finally, an outer film of cyclodextrin (CD) was formed electrochemically via Bulk electrolysis (the optimized method). The potential applied between the working electrode and the reference (Ag/AgCl) was held constant at +1.2 V for 3 min (the optimized time) in a solution of 10^{-5} M CD (the optimized concentration) in 0.05 M LiClO_4 . The proposed sensor is represented as Au/PEDOT/NF/CD.

2.4. Analysis of urine

The utilization of the proposed method in real sample analysis was also investigated by direct analysis of ACOP in human urine samples. ACOP was dissolved in urine to make a stock solution with 1 mmol L^{-1} concentration. Standard additions were carried out from the ACOP stock solution in 15 mL of 0.1 mol L^{-1} PBS (pH 7.40).

3. RESULT AND DISCUSSION

3.1. Electrochemistry of ACOP at Au/PEDOT/NF/CD

The electrochemistry of 1 mM ACOP/0.1 M PBS/pH 7.40 was studied at different modified electrodes (bare Au, Au/PEDOT, Au/PEDOT/NF, Au/PEDOT/CD and Au/PEDOT/NF/CD) as shown in (Fig. 1). An irreversible oxidation peak was observed at bare Au electrode at 508 mV with 9.2 μA anodic current. Upon modification with PEDOT (Au/PEDOT), the oxidation peak potential shifted negatively to 384 mV and the oxidation peak current increased to 32.8 μA . No peaks were observed at Au/PEDOT/NF for ACOP. On the other hand, the anodic peak potential shifted to 393 mV at Au/PEDOT/CD and the oxidation peak current increased to 23.1 μA . Upon modification of bare Au with PEDOT, NF and CD (Au/PEDOT/NF/CD), higher oxidation peak current 63.1 μA was observed at 429 mV (Table 1). The oxidation peak current of ACOP increased by 72 %, 60 % and 85 % at Au/PEDOT, Au/PEDOT/CD and Au/PEDOT/NF/CD, respectively compared to bare Au which indicates the catalytic oxidation of ACOP at the proposed composite. There is a synergistic effect between PEDOT polymer, NF and CD films (i.e.) a combining effect of every component in the composite, which resulted in enhanced oxidation peak current and improved electron transfer kinetics of ACOP at Au/PEDOT/NF/CD. The previous results could be explained as following; PEDOT film, acting as an electron mediator with a rich electron cloud, contained a distribution of hydrophobic (reduced) and hydrophilic (oxidized) regions and the hydrophobic ACOP^+ cations prefer to interact

with the more hydrophobic regions favoring reversible oxidation of ACOP (pKa of ACOP is 9.5 therefore it is positively charged at pH 7.4) [1, 2]. Moreover, the nafion film enhanced the surface preconcentration/accumulation of ACOP via ion-exchange and accumulations of ACOP in the hydrophilic regions or the ion channels of the nafion film.

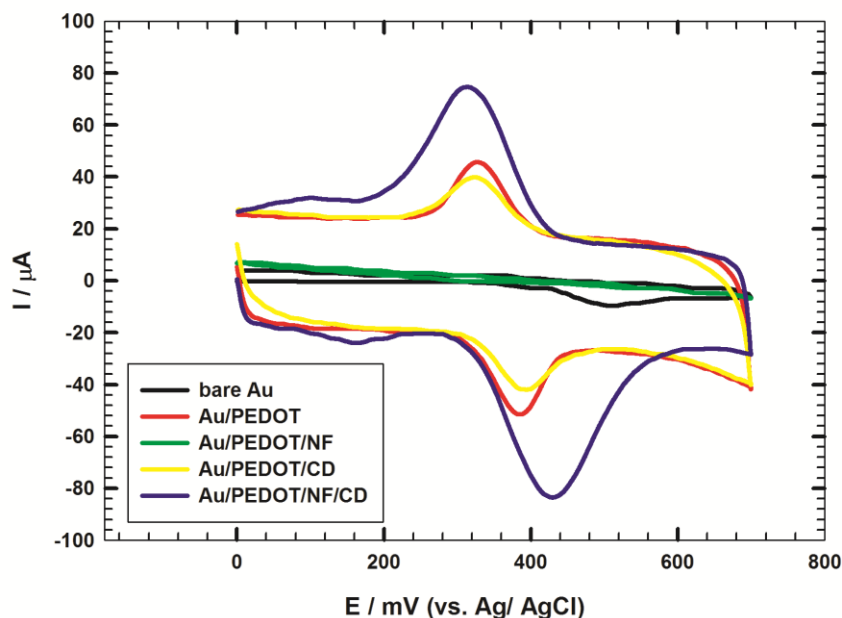


Figure 1. CVs of 1 mmol L^{-1} ACOP/ 0.1 mol L^{-1} PBS/pH 7.40 at bare Au, Au/PEDOT, Au/PEDOT/NF, Au/PEDOT/CD and Au/PEDOT/NF/CD, scan rate 50 mV s^{-1} .

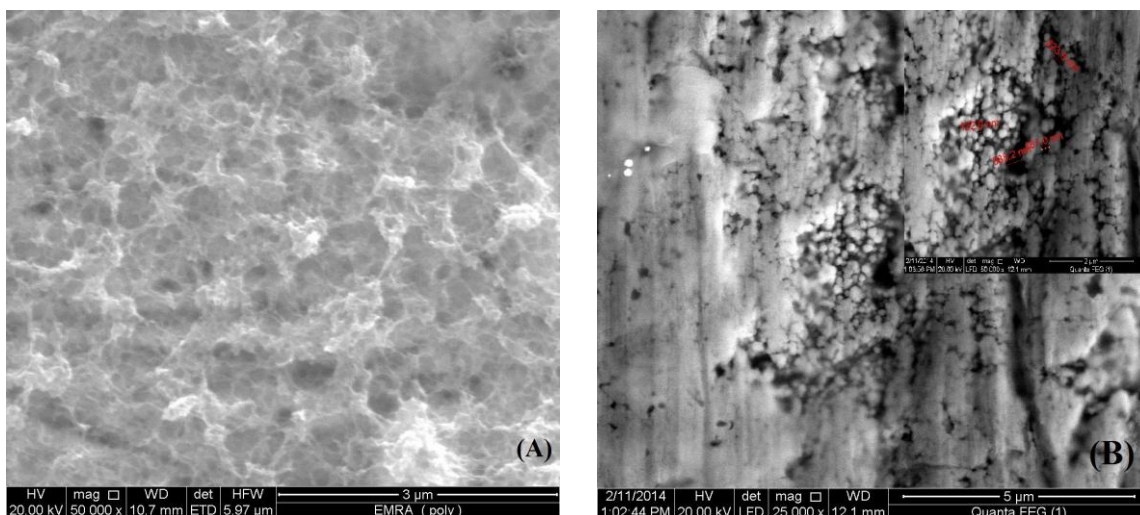
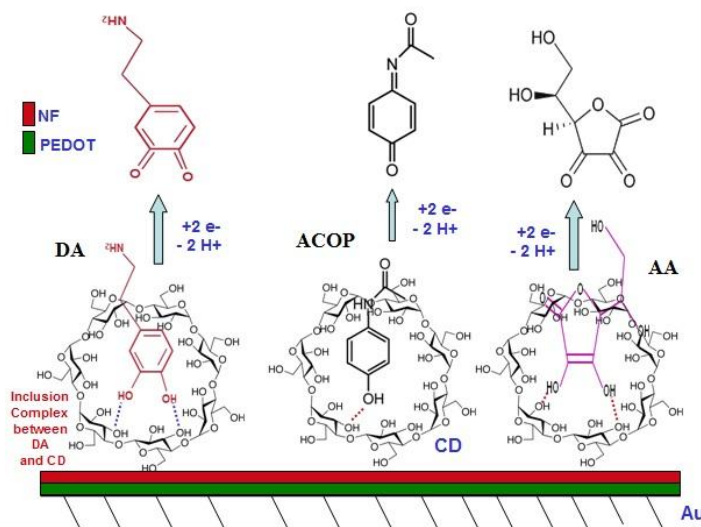


Figure 2. SEM micrographs of (A) Au/PEDOT with 50,000 magnification, (B) Au/PEDOT/NF/CD with 25,000 magnification, inset; greater magnification 50,000.

Improvement in the selectivity and sensitivity was achieved at the nafion film coated electrode [38-41]. In addition, nafion improves the electrical conductivity of the composite as well it works as

suitable layer for the formation of the CD film over it due to its good adhesion at the polymer surface and good film forming ability. By the modification of Au/PEDOT/NF with CD film, enhanced charge transfer kinetics and improved oxidation current for ACOP were obtained. A supramolecular host-guest inclusion complex is formed between β -CD and ACOP via electrostatic, inclusion interactions and hydrogen bonds formation (Scheme 1). The formation of such complex resulted in selectivity advantage and enhancement of the charge transfer properties of ACOP. ACOP molecules penetrate into the less polar cavity of β -CD and ACOP:CD inclusion complex was formed which further resulted in significant increase in oxidation signal of ACOP.

The physical morphology of the surface affected the response of an electrochemical sensor. An obvious difference was observed between Au/PEDOT and Au/PEDOT/NF/CD as shown in Fig. 2 (A, B); respectively. PEDOT film (Fig. 2A) has globular morphology and the surface looks rough due to the Au substrate. On the other hand, Au/PEDOT/NF/CD (Fig. 2B) showed unique morphology with highly porous surface which resulted in greater specific surface area, enhanced contact area with the analyte, faster electron transfer and higher catalytic activity.



Scheme 1. Schematic representation of the inclusion complex formation between CD and ACOP, AA and DA as guest molecules.

Table 1. Summary of CV results obtained at different modified electrodes for 1 mmol L^{-1} ACOP in 0.1 mol L^{-1} PBS/pH 7.40, scan rate 50 mV s^{-1} .

Electrode	E_{pa} mV	I_{pa} μA	ΔE mV	D_{ox} cm^2/s
Bare Au	508	9.2	---	9.34×10^{-6}
Au/PEDOT	384	32.8	56	1.19×10^{-4}
Au/PEDOT/CD	393	23.1	65	5.89×10^{-5}
Au/PEDOT/NF/CD	429	63.1	114	4.39×10^{-4}

E_{pa} ; the anodic peak potential, I_{pa} ; the anodic peak current, ΔE ; the potential peak separation, D_{app} ; the apparent diffusion coefficient.

3.2. Effect of accumulation time

The accumulation time is an important factor affecting the sensitivity of the proposed method. Fig. 3 showed the effect of the accumulation time from 0 to 80 s on the oxidation peak currents of ACOP at Au/PEDOT/NF/CD. The oxidation peak currents of ACOP increased sharply within the first 20 s reaching a maximum value. With further increasing accumulation time, the oxidation peak current decreased at 40 s then reached a constant value. Therefore, the optimum accumulation time used in this study is 20 s [35].

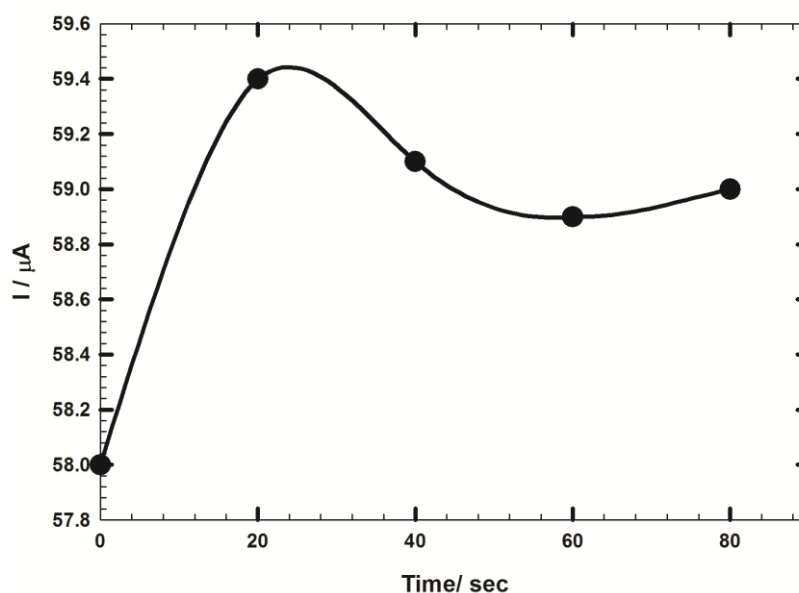


Figure 3. Effect of accumulation time of ACOP at Au/PEDOT/NF/CD from 0 to 120 s (current $I/\mu\text{A}$ against time t/s).

3.3. Effect of scan rate

The effect of the scan rate on the anodic peak current (I_{pa} A) was used for the estimation of the “apparent” diffusion coefficient D_{app} of 1 mM ACOP/0.1 M PBS/pH 7.40. D_{app} ($\text{cm}^2 \text{s}^{-1}$) values were calculated from Randles Sevcik equation:

$$I_{\text{pa}} = (2.69 \times 10^5) n^{3/2} A C_0 D^{1/2} v^{1/2}$$

where n is the number of electrons exchanged in oxidation at $T = 298 \text{ K}$, A is the geometrical electrode area = 0.0177 cm^2 , C_0 is the analyte concentration ($1 \times 10^{-6} \text{ mol cm}^{-3}$) and v is the scan rate V s^{-1} . It is important to notice that the apparent surface area used in the calculations does not take into account the surface roughness, which is inherent characteristic for all polymer films formed using the electrochemical techniques. Fig. 4 shows the CVs of 1 mmol L^{-1} ACOP/ 0.1 mol L^{-1} PBS/pH 7.40 at Au/PEDOT/NF/CD at different scan rates (from 10 mV s^{-1} up to 200 mV s^{-1}). The anodic and cathodic peak currents and the peak-to-peak separation increased and the anodic peak potential shifted to more positive value with increasing the scan rate. On the other hand, a plot of the anodic peak

current values of ACOP at Au/PEDOT/NF/CD versus the square root of the scan rate results in a straight-line relationship indicating that the oxidation process of ACOP is a diffusion-controlled process (the inset of Fig. 4). D_{app} values are 9.34×10^{-6} , 1.19×10^{-4} , 5.89×10^{-5} and 4.39×10^{-4} at bare Au, Au/PEDOT, Au/PEDOT/CD and Au/PEDOT/NF/CD, respectively (Table 1). These values indicate the enhanced charge transfer rate and the catalytic ACOP oxidation at the proposed composite.

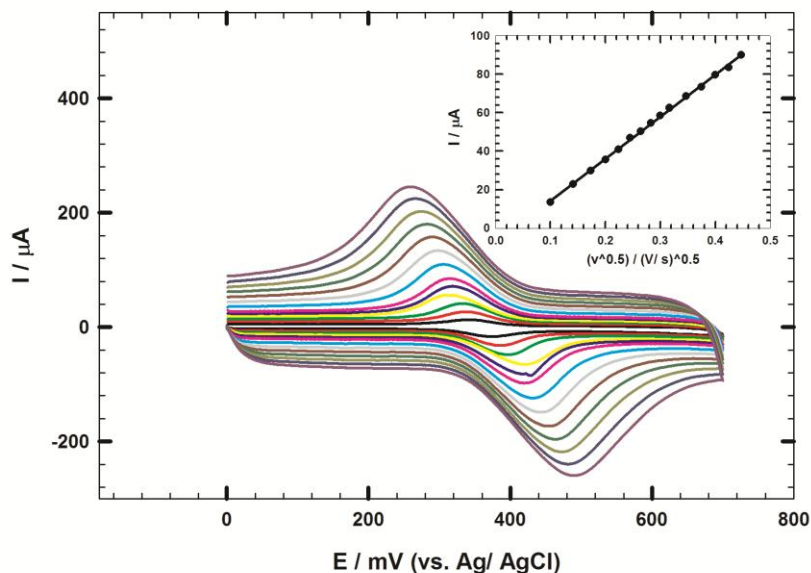


Figure 4. CVs of 1 mmol L^{-1} of ACOP/ 0.1 mol L^{-1} PBS/pH 7.40 at Au/PEDOT/NF/CD at different scan rates ($10\text{--}200 \text{ mV s}^{-1}$), the inset; linear relationship of I_{pa} vs. $v^{1/2}$.

3.4. Effect of solution pH

The electrochemical response of ACOP was affected by changing the pH of the supporting electrolyte (Fig. 5). The peak potentials and the peak currents of ACOP were affected by changing the pH of the supporting electrolyte. With increasing the solution pH, both the anodic and the cathodic peak potentials of ACOP shifted negatively. This indicated that the electrocatalytic oxidation of ACOP at Au/PEDOT/NF/CD is a pH-dependent reaction and protons processes are taking part in the charge transfer process. The relationship between the anodic peak potential and the solution pH value (over the pH range of 2–11) could be fit to the linear regression equation with a correlation coefficient of $R^2 = 0.992$ (inset of Fig. 5),

$$E_{pa} (\text{V}) = (0.8) - (0.0496) \text{ pH}$$

The slope was -0.0496 V/pH units over the pH range 2–11, which is close to the theoretical value of -0.059 V/pH . This indicated that the number of protons and transferred electrons involved in the oxidation mechanism is equal. As the ACOP oxidation is a two-electron process, the number of protons involved was also predicted to be two indicating a $2e^-/2H^+$ process [2, 4, 10]. On the other hand, the anodic peak current decreased from pH 2 to pH 5, then increased to pH 7.4 where it reached its maximum value and decreased again at pH 11.00 (Fig. 5). The highest oxidation peak current was

obtained at pH 7.40 (pH medium of the human body) therefore pH 7.40 is taken as the optimum pH for this study.

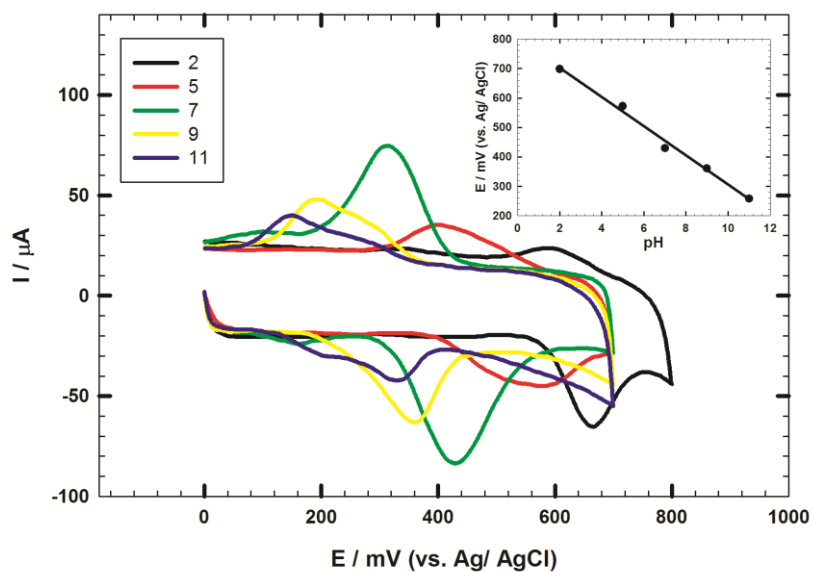


Figure 5. CVs of 1 mmol L⁻¹ of ACOP/0.1 mol L⁻¹ PBS with different pH values (2-11) at Au/PEDOT/NF/CD, inset; linear relationship between the anodic peak potential (mV) vs. the pH values, scan rate 50 mV s⁻¹.

3.5. Stability of the proposed sensor

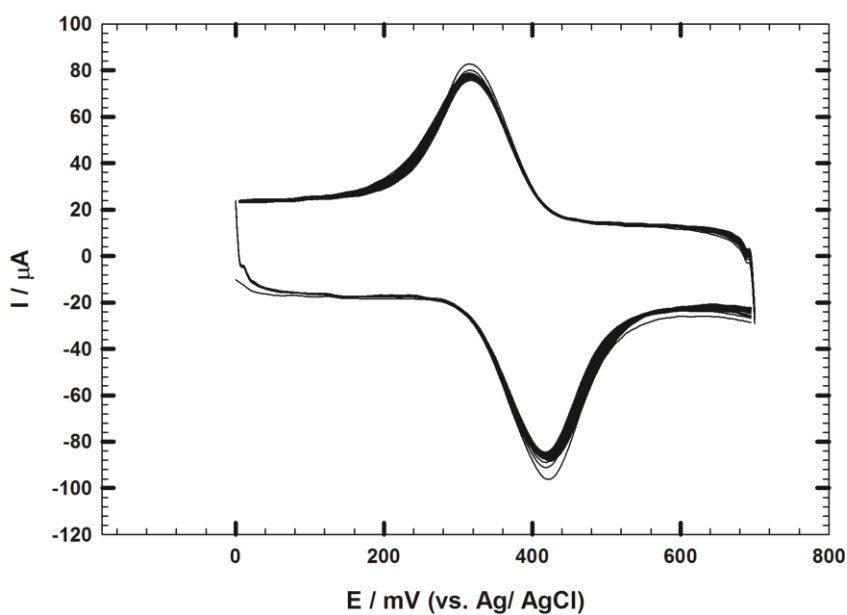


Figure 6. Stability of Au/PEDOT/NF/CD for 1 mmol L⁻¹ of ACOP/0.1 mol L⁻¹ PBS/pH 7.40, 25 repeated cycles, scan rate 50 mV s⁻¹.

The stability of the proposed sensor; Au/PEDOT/NF/CD was studied via repeated cycles up to 25 cycles in 1 mmol L⁻¹ ACOP/0.1 mol L⁻¹ PBS/pH 7.4 as shown in (Fig. 6). Excellent stability without any noticeable decrease in the current response and no change in the oxidation peak potential was obtained. As a result, this modified electrode has good stability and does not suffer from surface fouling during the repetitive voltammetric measurement. Thus, the proposed sensor exhibited enhanced catalytic activity and good stability.

3.6. Determination of ACOP at physiological pH using Au/PEDOT/NF/CD

Differential pulse voltammetry (DPV) was used to investigate the voltammetric behavior of ACOP at Au/PEDOT/NF/CD. The inset of (Fig. 7) shows typical DPV of standard additions of 0.5 mmol L⁻¹ ACOP/0.1 mol L⁻¹ PBS/pH 7.40 in 15 mL of 0.1 mol L⁻¹ PBS/pH 7.40 at Au/PEDOT/NF/CD.

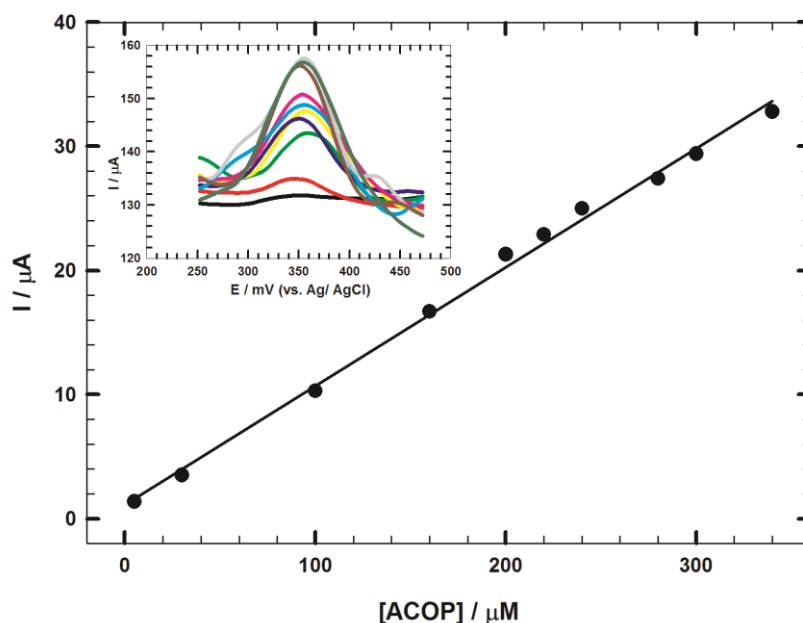


Figure 7. Calibration curve for ACOP for concentrations from 5 μmol L⁻¹ to 340 μmol L⁻¹. Inset: DPVs of standard additions of 0.5 mmol L⁻¹ ACOP/0.1 mol L⁻¹ PBS/pH 7.40 in 15 ml of 0.1 mol L⁻¹ PBS/pH 7.40 at Au/PEDOT/NF/CD

It is observed that by increasing the concentration of ACOP, the anodic peak current increases indicating the improvement of the electrochemical response of ACOP at Au/PEDOT/NF/CD due to the enhanced accumulation of protonated ACOP. Fig. 7 shows the calibration curve of the anodic peak current values in the linear range of 5–340 μmol L⁻¹ ACOP with the regression equation:

$$I_p (\text{A}) = (1.121 \times 10^{-6}) + 9.572 \times 10^{-8} c (\mu\text{mol L}^{-1})$$

and with correlation coefficient of 0.9961, sensitivity of 0.0957 μA/μmol L⁻¹ and detection limit of 15.7 nmol L⁻¹. The detection limit (DL) was calculated from:

$$DL = 3s/b$$

where s is the standard deviation and b is the slope of the calibration curve. Table 2 shows the comparison for the determination of ACOP at Au/PEDOT/NF/CD with various modified electrodes based in literature reports. The proposed sensor showed the excellent features, such as wide linear response range, high sensitivity and selectivity, good reproducibility and long time stability.

Table 2. Comparison for determination of ACOP at various modified electrodes-based literature reports.

Electrode	LDR (μM)	pH	Sensitivity ($\mu\text{A}/\mu\text{M}$)	LOD (nM)	Reference
AuNps-Nafion/CP	0.05-50	7.4	0.0619	7.7	2
Nafion/TiO ₂ -GR/GCE	1-100	7	0.3472	210	5
MIP	1-4000	7	0.0502	330	6
Graphene/GCE	0.1-20	7	4.055	32	9
MCM-CPE	0.5- 2200	7	0.090	60	12
GCE/MWCNT-Polyhis	0.25-10	7	0.63	32	13
Au/PEDOT/NF/CD	5-340	7.4	0.0957	15.7	This work

LDR; Linear dynamic range, AuNps; gold nanoparticles, GR; graphene, GCE; glassy carbon electrode, MIP; molecular imprinted polymeric micelle, MCM-CPE; MCM-41 modified carbon paste electrode, GCE/MWCNT-Polyhis; glassy carbon electrode modified with multi-wall carbon nanotubes dispersed in polyhistidine.

3.7. Determination of ACOP in human urine samples

The application of the proposed sensor in real sample analysis was also studied by direct analysis of ACOP in human urine. The same measurements were conducted successfully on urine samples. In this set of experiments, ACOP was dissolved in urine to make a stock solution with 0.5 mmol L^{-1} concentration. The detection limit of 36.1 nmol L^{-1} with correlation coefficient 0.9958 of is obtained in the linear range of $3\text{-}300 \mu\text{mol L}^{-1}$ (Fig. 8). Four different concentrations on the calibration curve are chosen to be repeated to evaluate the accuracy and precision of the proposed method, which is represented in (Table 3). The recovery ranged from 99 % to 100.5 %, and the results are acceptable indicating that the present procedures are free from interferences of the urine sample matrix. The results strongly proved that ACOP can be selectively and sensitively determined at Au/PEDOT/NF/CD modified electrode in urine sample. This sensor proved to be successfully used for ACOP determination in pharmaceutical and clinical preparations.

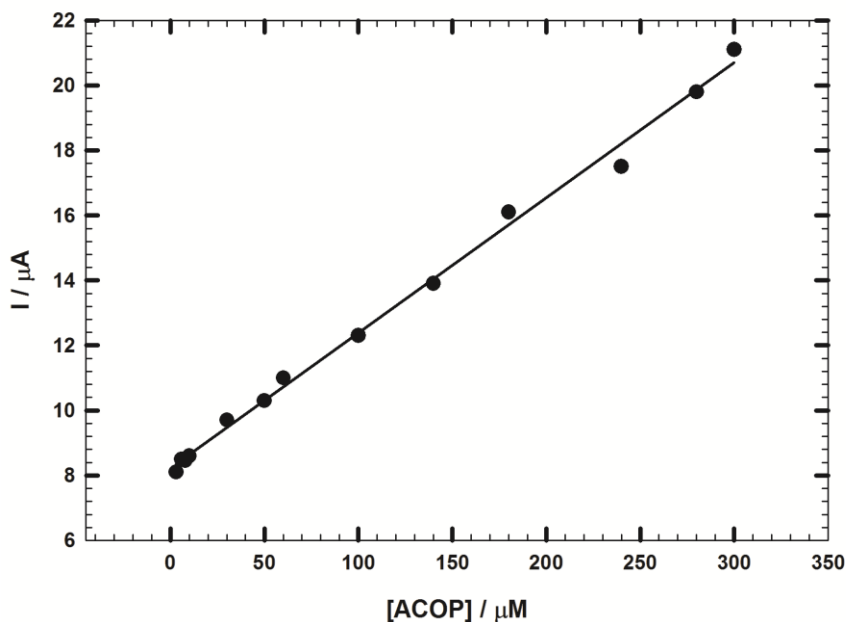


Figure 8. Calibration curve of ACOP in urine at Au/PEDOT/NF/CD for concentrations from 3 μmol L⁻¹ to 300 μmol L⁻¹.

Table 3. Evaluation of the accuracy and precision of the proposed method for the determination of ACOP in urine sample.

Sample	Concentration of ACOP added (μmol L ⁻¹)	Concentration of found ACOP (μmol L ⁻¹) ^a	Recovery (%)	Standard deviation × 10 ⁻⁷	Standard error × 10 ⁻⁸
1	8	7.97	99.6	1.041	6.009
2	50	49.5	99	1.000	5.774
3	140	140.5	100.5	1.041	6.009
4	280	281.4	100.5	1.000	5.774

^a Average of five determinations.

3.8. Effect of interferences on the determination of ACOP

Au/PEDOT/NF/CD sensor was evaluated for the simultaneous voltammetric determination of ACOP and different neurotransmitters (DA, EP, NE) in binary and tertiary mixtures [1-3, 12]. Figure 9 (A) showed the DPVs of 1 mM ACOP and 1 mM EP/0.1 M PBS/pH 7.4 at Au/PEDOT/NF/CD. The inset showed the DPVs of 1 mM ACOP and 1 mM NE/0.1 M PBS/pH 7.4 at Au/PEDOT/NF/CD. Two well resolved peaks were obtained at 200 mV and 380 mV for EP and ACOP and at 200 mV and 390 mV for NE and ACOP, respectively. On the other hand, ACOP is likely to interfere with DA and AA determination in biological samples [1-3, 7, 8, 13]. Figure 9 (B) showed the DPVs of 1 mM ACOP, 1

mM DA and 1 mM AA/0.1 M PBS/pH 7.4 at Au/PEDOT/NF/CD. The inset showed the DPVs of 1 mM ACOP, 1 mM EP and 1 mM AA/0.1 M PBS/pH 7.4 at Au/PEDOT/NF/CD. Three well separated oxidation peaks with good potential peak separation were obtained in the two cases. These results indicated the validity and performance of the proposed sensor for the simultaneous determination of ACOP in the presence of the interfering species in the biological fluids with large peak separation and high sensitivity.

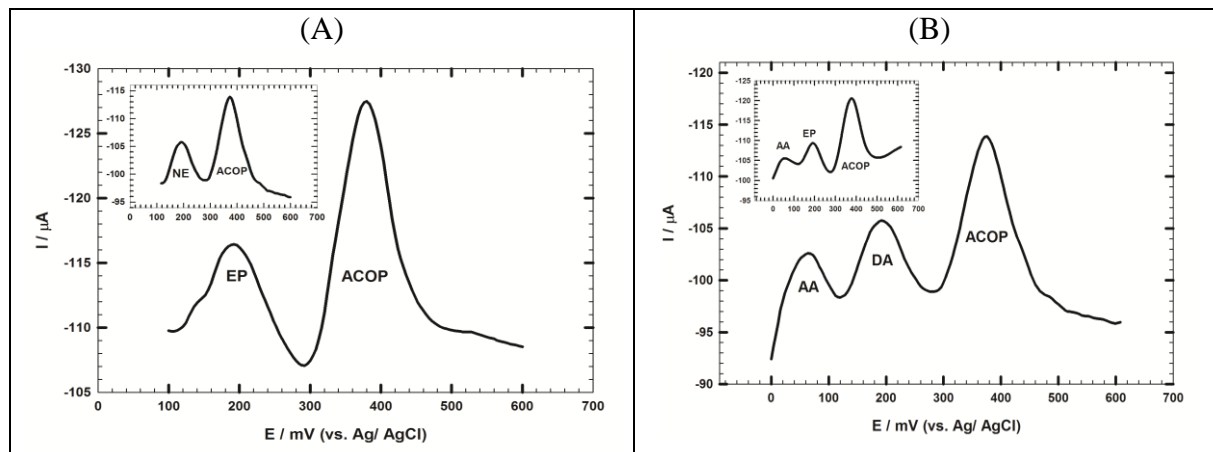


Figure 9. (A) DPVs of 1 mmol L⁻¹ ACOP in the presence of 1 mmol L⁻¹ EP at Au/PEDOT/NF/CD in the mixture solution (0.1 mol L⁻¹ PBS/pH 7.40), the inset; DPVs of 1 mmol L⁻¹ ACOP in the presence of 1 mmol L⁻¹ NE at Au/PEDOT/NF/CD. (B) DPVs of 1 mmol L⁻¹ ACOP in the presence of 1 mmol L⁻¹ AA and 500 μmol L⁻¹ DA at Au/PEDOT/NF/CD in the mixture solution (0.1 mol L⁻¹ PBS/pH 7.40), the inset; DPVs of 1 mmol L⁻¹ ACOP in the presence of 1 mmol L⁻¹ AA and 500 μmol L⁻¹ EP at Au/PEDOT/NF/CD.

3.9. Electrochemical Impedance Spectroscopy

Electrochemical impedance spectroscopy (EIS) can be used to investigate the interface properties of the modified surface. EIS data were obtained at ac frequency varying between 0.1 Hz and 100 kHz. The EIS measurements were carried out in a solution of 1 mM ACOP in 0.1 M PBS/ pH 7.40 at 508 mV and 430 mV; the oxidation potentials of ACOP at bare and modified electrode, respectively. Fig. 10 showed the typical impedance spectra presented in the form of Nyquist plot for modified and bare electrodes. The experimental data were compared to an equivalent circuit that used some of the conventional circuit elements (inset of Fig. 10). In this circuit, R_s is the solution resistance and R_{ct} is the charge transfer resistance. CPE1 and CPE2 represent the predominant diffusion influence on the charge transfer process and n and m are their corresponding exponents (n and m less than one). C_f and C_c represent the capacitance of the double layer and W is the Warburg impedance due to diffusion. Table 4 lists the best fitting values calculated from the equivalent circuit for the impedance data.

The semicircle diameter in the impedance spectrum represents the interfacial electron transfer resistance R_{ct} . This resistance controls the electron transfer kinetics of the redox probe at the electrode interface and can be used to describe the interface properties of the electrode. R_{ct} equals 7026 Ω cm² in case of bare Au which decreases greatly (1981 Ω cm²) in the case of the proposed sensor. This

noticeable decrease in the Rct value indicated less electronic resistance and more facilitation of charge transfer. The Au/PEDOT/NF/CD modified sensor played an important role in the obvious decrease of interfacial electron transfer resistance Rct.

As well, the value of Warburg impedance due to diffusion (W) for bare Au is $1.71 \times 10^4 \Omega s^{-1/2}$ which decreases greatly to $5.45 \times 10^3 \Omega s^{-1/2}$ for modified electrode, indicating less electronic resistance and more facilitation of charge transfer. On the other hand, the capacitive component of the charge at the modified electrode is relatively higher compared to that at the bare Au (Table 4). This is due to the increase in the ionic adsorption at the electrode/electrolyte interface.

Table 4. EIS fitting data corresponding to Fig. 10 for bare electrode and the proposed sensor.

	R_s Ωcm^2	C_c $F cm^{-2}$	R_{ct} Ωcm^2	W $\Omega s^{-1/2}$	$CPE1$ $F cm^{-2}$	n	C_f $F cm^{-2}$	$CPE2$ $F cm^{-2}$	m
Bare Au	8833	2.51×10^{-10}	7026	1.71×10^4	1.32×10^4	0.2333	5.72×10^{-5}	4.37×10^4	0.805
Sensor	285	1.79×10^{-9}	1981	5.45×10^3	1.21×10^4	0.7314	2.37×10^{-4}	1.25×10^2	0.225

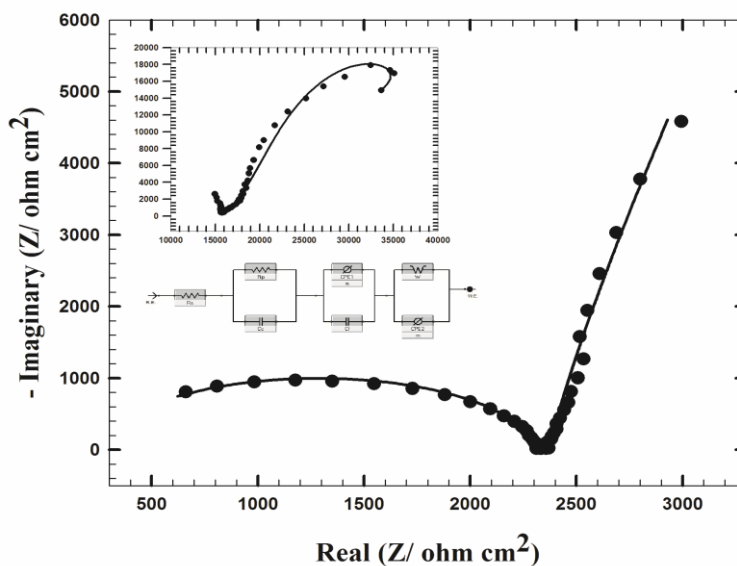


Figure 10. Nyquist plot of Au/PEDOT/NF/CD and bare Au in 1 mmol L^{-1} of ACOP/ 0.1 mol L^{-1} PBS/pH 7.40 at the oxidation potential of ACOP mV. (Symbols and solid lines represent the experimental measurements and the computer fitting of impedance spectra, respectively), frequency range: 0.1–100 000 Hz. Inset, the equivalent circuit used in the fit procedure of the impedance spectra.

4. CONCLUSIONS

Conducting PEDOT polymer film, nafion and cyclodextrin have been utilized to construct nanocomposite to be used as sensor for paracetamol. A supramolecular host-guest inclusion complex is

formed between β -CD and ACOP via electrostatic, inclusion interactions and hydrogen bonds formation. So Au/PEDOT/NF/CD modified sensor explores a very good synergism between PEDOT matrix, NF and CD to promote surface preconcentration, faster electron transfer and higher electrocatalytic activity towards the electrooxidation of paracetamol. The proposed sensor, Au/PEDOT/NF/CD, was successfully used to determine ACOP in presence AA and UA as common interferences in biological fluids. In addition, this method was successfully applied for determination of ACOP in human urine samples with good precision, accuracy, and relatively low detection limit of 36.1 nmol L^{-1} in the linear dynamic range of $3\text{--}300 \text{ }\mu\text{mol L}^{-1}$. The simultaneous determinations of ACOP and epinephrine (EP), ACOP and norepinephrine (NE), ACOP, DA and AA and ACOP, EP and AA were done with high resolution and good potential peak separation.

ACKNOWLEDGEMENT

The authors would like to acknowledge the financial support from Cairo University through the Vice President Office for Research Funds.

References

1. N.F. Atta, A. Galal and S.M. Azab, *Int. J. Electrochem. Sci.*, (6) (2011) 5082.
2. N.F. Atta, A. Galal, F.M. Abu-Attia and S.M. Azab, *J. Mater. Chem.*, (21) (2011) 13.
3. N.F. Atta, M.F. El-Kady and A. Galal, *Sens. Actuators B*, 141 (2009) 566.
4. L. Junhua, JinlongLiu, GongrongTan, JianboJiang, SanjunPeng, MiaoDeng, Q. Dong, YonglanFeng and YoucaiLiu, *Biosens. Bioelectron.*, 54 (2014) 468.
5. Y. Fa, J. Liu J, H. Lu and Q. Zhang, *Colloids Surf. B*, 85 (2011) 289.
6. J. Luo, C. Fan, X. Wang, R. Liu and X. Liu, *Sens. Actuators B*, 188 (2013) 909.
7. A.T.E. Vilian, M. Rajkumar and S. Chen, *Colloids Surf. B*, 115 (2014) 295.
8. S. Cheemalapati, S. Palanisamy, V. Mani and S. Chen, *Talanta*, 117 (2013) 297.
9. X. Kang, J. Wang, H. W. J. Liu, I.A. Aksay and Y. Lin, *Talanta*, 81 (2010) 754.
10. M. Arvand and T.M. Gholizadeh, *Colloids Surf. B*, 103 (2013) 84.
11. L. Özcan and Y. Şahin, *Sens. Actuators B*, 127 (2007) 362.
12. M.M. Ardakani, M.A.S. Mohseni, M.A. Alibeik and A. Benvidi, *Sens. Actuators B*, 171–172 (2012) 380.
13. P.R. Dalmasso, M.L. Pedano and G.A. Rivas, *Sens. Actuators B*, 173 (2012) 732.
14. B. Rajesh, K.R. Thampi, J.M. Bornard, A.J. McEvoy, N. Xanthopoulos, H.J. Mathieu and B. Viswanathan, *J. Power Sources*, 133 (2004) 155.
15. X. Huang, Y. Li, Y. Chen and L. Wang, *Sens. Actuators B*, 134 (2008) 780.
16. C.Y. Lin, V.S. Vasantha and K.C. Ho, *Sens. Actuators B*, 140 (2009) 51.
17. F.S. Belaidi, D. Evrard and P. Gros, *Electrochem. Commun.*, 13 (2011) 423.
18. N.F. Atta, A. Galal and R.A. Ahmed, *Bioelectrochemistry*, 80 (2011) 132.
19. A. Kros, N.A.J.M. Sommerdijk and R.J.M. Nolte, *Sens. Actuators B*, 106 (2005) 289.
20. A.R. Gonçalves, M.E. Ghica and C.M.A. Brett, *Electrochim. Acta*, 56 (2011) 3685.
21. F.S. Belaidi, P.T. Boyer and P. Gros, *J. Electroanal. Chem.*, 647 (2010) 159.
22. H.C. Yi, K.B. Wu, S.S. Hu and D.F. Cui, *Talanta*, 55 (2001) 1205.
23. P. Luo, G. Xie, Y. Liu, H. Xu, S. Deng and F. Song, *Clin. Chem. Lab. Med.*, 46 (2008) 1641.
24. P.Y. Chen, R. Vittal, P.C. Nien and K.C. Ho, *Biosens. Bioelectron.*, 24 (2009) 3504–3509.
25. G. Nagy, G.A. Gerhardt, A.F. Oke, M.E. Rice, R.N. Adams, M.N. Szentirmay and C.R. Martin, *J. Electroanal. Chem.*, 188 (1985) 85.

26. Y. Chen and T.C. Tan, *Talanta*, 42 (1995) 1181.
27. M.M. Dávila, M.P. Elizalde, J. Mattusch and R. Wennrich, *Electrochim. Acta*, 46 (2001) 3189.
28. S. Yuan and S. Hu, *Electrochim. Acta*, 49 (2004) 4287.
29. C.G. Caridade and C.M.A. Brett, *Electroanalysis*, 17 (2005) 549.
30. S.Tan and D. Bélanger, *J. Phys. Chem. B*, 109 (2005) 23480.
31. T. Lu and I. Sun, *Electroanalysis*, 12 (2000)605.
32. N.F. Atta, A.Galal and S.M. Azab, *J. Electrochem. Soc.*, 159 (10) (2012) H765.
33. N.F. Atta, A. Galal and S.M. Azab, *Analyst*, 136 (2011) 4682.
34. N.F. Atta, A. Galal, F.M. Abu-Attia and S.M. Azab, *J. Mater. Chem.*, 21 (2011) 13015.
35. D.P. Quana, D.P. Tuyena, T.D. Lamb, P.T.N. Trama, N.H. Binh and P.H. Viet, *Colloids Surf. B*, 88 (2011) 764.
36. A. Babaei and A.R. Taheri, *Sens. Actuators B*, 176 (2013) 543.
37. S. Ku, S. Palanisamy and S. Chen, *J. Colloid Interface Sci.*, 411 (2013) 182.
38. X. Tian, C. Cheng, H. Yuan, J. Dua, D. Xiao, S. Xie and M.M.F. Choi, *Talanta*, 93 (2012) 79.
39. Y. Wu, Z. Dou, Y. Liu, G. Lv, T. Pu, X. He, *RSC Adv.*, 3 (2013) 12726.
40. D. Jia D, J. Daib, H. Yuana, L. Lei and D. Xiao, *Talanta*, 85 (2011) 2344.
41. M.L. Bender and M. Komiyama, *Cyclodextrin Chemistry*, Springer-Verlag, Berlin, Heidelberg, New York, (1978) 701.
42. W. Saenger and J.S. Zejtli, *Proceedings of the First International Symposium on Cyclodextrin*, D. Reidel Publishing Company Press, Hungary, (1982) 141.
43. P. He, J. Ye, Y. Fang, I. Suzuki, and T. Os, *Anal. Chim. Acta*, 337: (1997) 217.
44. A. Ferancová, E. Korgová, T. Buzinkaiová, W. Kutner, I. Štěpánek and J.Labud, *Anal. Chim. Acta*, 447(2001) 47.
45. Y. Hu, Z. Zhang, H. Zhang, L. Luo and S. Yao, *Talanta*, 84 (2011)305.
46. A. Ueno, I. Suzaki and T. Osa, *Anal. Chem.*, 62 (1990) 2461.
47. A. Abbaspour and A. Noori, *Biosens. Bioelectron.*, 26 (2011) 4674.
48. A.J. Bard and L.R. Falkner, *Electrochemical Methods, Fundamentals and Applications*, (2001) Wiley, New York.
49. C.C. Harley, A.D. Rooney and C.B. Breslin, *Sens. Actuators B*, 150 (2010) 498.
50. G.A. Angeles, B.P. López, M.E.P. Pardave, M.T.R. Silva, S. Alegret and A. Merkoçi, *Carbon*, 46 (2008) 898.
51. M.T.R. Silva, S.C.S. Avendaño, G.A. Angelesc, A.R. Hernández, M.A. Romero-Romo and Pardavé MP, *ECS Trans.*, 20 (1) (2009) 151.
52. M.P. Pardavé, G.A. Angelesc, S.C.S. Avendaño, M.A. Romero-Romo, A. Merkoçi, A.R. Hernández and M.T.R. Silva, *ECS Trans.*, 36 (1) (2011) 471.
53. W. Lian, J. Huang, J. Yu, X. Zhang, Q. Lin, X. He, X. Xing and S.Liu, *Food Control*, 26 (2012) 620.
54. D. Bouchta, N. Izaoumen, H. Zejli, M. El-Kaoutit and K.R. Temsamani, *Biosens. Bioelectron.*, 20 (2005) 2228.
55. X. Xu, Z. Liu, X. Zhang, S. Duan, S. Xu and C. Zhou, *Electrochim. Acta*, 58 (2011) 142.
56. H. Wanga, Y. Zhou, Y. Guo, W. Liu, C. Dong, Y. Wu, S. Li and S.Shuang, *Sens. Actuators B*, 163 (2012) 171.
57. A. Cao, H. Ai, Y. Ding, C. Dai and J. Fei, *Sens. Actuators B*, 155 (2011) 632.
58. N. F. Atta, A.Galal, S. M. Ali and D. M. El-Said, *Anal. Methods*, 6 (2014) 5962.
59. J. Han, K. Huang, J. Li, Y. Liu and M. Yu, *Colloids Surf. B*, 98 (2012) 58.